Produced Water Treatment by Micellar-Enhanced Ultrafiltration

ARTICLE *in* ENVIRONMENTAL SCIENCE AND TECHNOLOGY · MARCH 2010

Impact Factor: 5.33 · DOI: 10.1021/es902862j · Source: PubMed

3 AUTHORS, INCLUDING:

Maen M. Husein
The University of Calgary
51 PUBLICATIONS **588** CITATIONS

SEE PROFILE

Environ. Sci. Technol. **2010,** *44,* 1767–1772

Produced Water Treatment by Micellar-Enhanced Ultrafiltration

ALI DERISZADEH, MAEN M. HUSEIN,* AND THOMAS G. HARDING

Department of Chemical & Petroleum Engineering, University of Calgary 2500 University Drive NW, Calgary, Alberta, Canada T2N 1N4

Received September 21, 2009. Revised manuscript received January 19, 2010. Accepted January 20, 2010.

A water treatment approach combining ultrafiltration (UF) and micellar-enhanced ultrafiltration (MEUF) techniques was used for the removal of organic contaminants in field produced water samples from Canada and the United States. Free oil droplets and suspended solids were separated by initial UF treatments while MEUF was necessary for the removal of dissolved organics. It was shown that the amphiphilic characteristics of some organics commonly existing in produced water contributed to lowering the critical micelle concentration (CMC) of the surfactant employed. Lower surfactant concentrations could, therefore, be employed leading to lower fouling and back contamination and higher permeate flux. In addition, the incorporation of organic contaminants into the structure of cetylpyridinium chloride (CPC) micelles resulted in larger size and higher dissolution capacity of the "mixed micelles". The performance of polymeric and ceramic membranes of different molecular weight cutoffs (MWCOs) was evaluated by analyzing the permeate flux, recovery ratio, and solute percent rejection as functions of trans-membrane pressure (TMP). A mathematical model based on Darcy's law and the resistance in-series model successfully described the flux decline as a function of TMP for the two field samples and the two membranes studied.

Introduction

Produced water is by far the largest contaminated stream resulting from thermal heavy oil recovery operations (*1*) and its treatment and reuse is essential for the sustainability of oil sands processing (*2*). Organic contaminants in produced waters are toxic and corrosive leading to environmental and operational problems. From an environmental sustainability perspective, it is necessary to recycle produced water and thus it must undergo proper treatment in order to avoid potentially negative impacts on drinking water supplies and aquatic organisms (*3, 4*). From an industrial standpoint, the different contaminants in the produced water may adversely affect equipment leading to scaling and corrosion (*4*−*6*).

Micellar-enhanced ultrafiltration (MEUF) is a relatively low energy treatment process aimed at increasing the size of contaminant molecules by binding or dissolving them into micelles formed with an appropriate surfactant before the membrane separation step (*7*−*20*). MEUF could potentially be applied to treat produced water, especially when only low surfactant dosage is required. Low surfactant concentration enables appreciably higher permeate flux and lowers back contamination. One strategy of achieving low surfactant concentration during MEUF is to lower the critical micelle concentration (CMC) of an ionic surfactant by addition of nonionic surfactant (*21*−*23*). In previous work involving synthetic produced waters (*7, 8*), we showed that naphthenic acid cocontaminants participated in forming "mixed micelles" and led to lowering the CMC of cetylpyridinium chloride (CPC) while increasing its contaminant solubilization capacity. In the current investigation, the applicability of our previous findings to field produced waters from Alberta (Canada) and California was examined. Moreover, the applicability of a mathematical model based on Darcy's law and a resistance in-series model to describe the permeate flux for the two field samples filtered through either polymeric or ceramic membranes was evaluated.

Materials and Methods

Chemicals. Cetylpyridinium chloride, CPC, (99 wt. % pure, Fisher Scientific, ON) was used as the cationic surfactant for the MEUF runs. Two field water samples from oil production sites were obtained from Alberta (Canada), sample A, and California, sample B.

Membranes. Hollow fiber polyacrylonitrile (PAN) polymeric (Pall Corporation, ON) and the channel structure titanium oxide (TiO_2) ceramic (Sterlitech Corporation, WA) membranes having different molecular weight cut-offs (MWCO) were used. The specifications of the membranes are listed in Table 1.

Experimental Procedure. The cross-flow MEUF setup was built as per the experimental approach previously employed for the synthetic water samples (*7*). However, pretreatment steps were deemed necessary in this case since the field samples contained suspended solids and free oil droplets. The treatment train was comprised of three steps. In step 1 a batch-wise ultrafiltration (UF) pretreatment using 50 kDa polymeric membrane was used. The permeate of the first step was fed to step 2, where a 50 kDa ceramic membrane was used to perform a batch-wise UF treatment. In step 3, CPC was added to the permeate stream from step 2 to give a final concentration of 10 mM CPC, which was the minimum concentration to ensure dissolution of the organic contaminants. Continuous cross-flow MEUF runs were then attempted using polymeric and ceramic membranes. In MEUF runs of step 3 the permeate stream, as shown in Figure 1, was recycled to the feed tank to achieve steady state operation. The regeneration of both polymeric and ceramic membranes, following each UF or MEUF run, was carried out following the procedure of Deriszadeh et al. (*7, 8*). Cleaning continued until the original DI-water flux was re-established.

TABLE 1. Specification for PAN Polymeric and TiO_2 Ceramic Membranes

polymeric membranes		ceramic membranes	
length (cm)	34.7	length (cm)	25
diameter of the membrane module (cm)	4.5	membrane OD (cm)	1.0
membrane effective surface area (m^2)	0.2	membrane effective surface area (m^2)	0.013
number of hollow fibers per module	~300	number of channels	7
hollow fiber wall thickness (cm)	~0.04	channels wall thickness (cm)	0.1
inner diameter of the hollow fibers (cm)	0.08		

* Corresponding author phone (403) 220-6691; fax (403) 282-3945; e-mail: maen.husein@ucalgary.ca.

10.1021/es902862j
Published on Web 02/02/2010

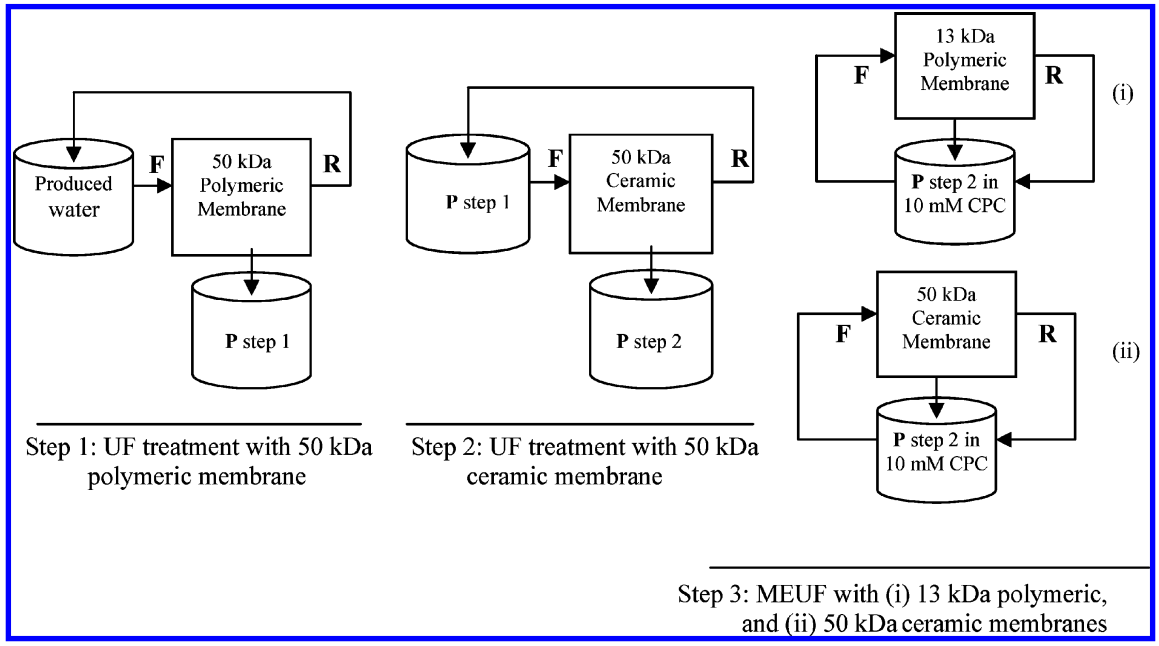

FIGURE 1. Treatment train for the removal of organic contaminants from produced water (F, feed; R, retentate; P, permeate).

The permeate flux, the percent rejection (%R), and the recovery ratio (r) were plotted as functions of trans-membrane pressure (TMP) for MEUF runs, whereas the permeate flux as a function of concentration factor was recorded during the UF batch-wise runs. Three independent runs were performed for all the experiments, and 95% confidence intervals are shown in the figures and tables. The trans-membrane pressure (TMP), the percent rejection (%R), the recovery ratio (r) and the concentration factor (CF) were calculated as follows:

$$\mathrm{TMP} = \frac{P_\mathrm{F} + P_\mathrm{R}}{2} \tag{1}$$

$$\%R = \left(1 - \frac{C_{i,\mathrm{P}}}{C_{i,\mathrm{F}}}\right) \times 100 \tag{2}$$

$$r = \frac{\dot{V}_\mathrm{P}}{\dot{V}_\mathrm{F}} \tag{3}$$

$$\mathrm{CF} = \frac{V_{\mathrm{F},0}}{V_{\mathrm{F},t}} \tag{4}$$

where, P_F and P_R are the gauge pressures from the feed and retentate sides, respectively, $C_{i,\mathrm{P}}$ and $C_{i,\mathrm{F}}$ are the concentration of solute i in the permeate and the feed sides, respectively, $\dot{V}_\mathrm{P}$ and $\dot{V}_\mathrm{F}$ are the volumetric flow rates of the permeate and the feed, respectively, and $V_{\mathrm{F},0}$ and $V_{F,t}$ are the volumes of the feed sample at time zero and time, t, following the start of the batch-wise UF runs.

Analyses. Gas chromatography, GC (HP 6890, Agilent Technologies, ON) was used to measure the concentration of CPC in the feed, permeate and retentate samples. An HP-5 GC column (30 m × 0.25 mm × 0.25 μm) (Agilent Technologies, ON) was used with helium as the carrier gas and GC oven temperature increasing from 80 to 230 at 10 °C/min, and maintained at 230 °C for 5 min. The injector and the flame ionization detector (FID) temperatures were fixed at 150 and 230 °C, respectively. The retention time of CPC ranged from 11.7 to 11.9 min. A 0.5 μL volume sample was injected into the GC. A total organic carbon analyzer, TOC (TOC-Ve, Mandel, ON) was used to measure the organic content of the field samples as received and following each UF treatment step, while a combination of TOC and GC measurements were used to evaluate solute concentrations during the MEUF runs. The difference between TOC and GC measurements, expressed as ppm, corresponded to the concentration of the organic contaminants. Three replicates were performed for every run, and the mean and the 95% confidence intervals were reported in the figures and tables.

A Krüss tensiometer (Krüss K12, Kruss Instruments, NC) was used to measure the critical micelle concentration (CMC) of the surfactant solution and the mixtures of the surfactant and the organic contaminants in the produced water samples (*7, 8*). Dynamic light scattering, DLS (Zetasizer, Nano series, Malvern Instruments, PA) was used to measure the size of colloidal suspensions in the raw water, CPC micelles as well as the "mixed micelles". A rotational rheometer/viscometer (HAAKE RotoVisco 1 Typo 003-5363, Thermo Scientific, MA) was used to measure the viscosities of the different water samples.

Results and Discussion

Step 1 Treatment. The existence of suspended solids and free oil droplets mandated an UF preliminary treatment step using a 50 kDa polymeric membrane. The choice of the membrane size was based on our previous results for synthetic produced water (*7, 8*) and size of colloidal suspensions in the raw water. DLS measurements of the raw produced water identified colloidal particles larger than 1.0 μm. This step was performed in a batch-wise mode and at a constant TMP of about 150 kPa.

The permeate of sample A following step 1 treatment was transparent, but with a pale yellow color. The TOC measurements showed that the UF treatment using the 50 kDa polymeric membrane reduced the dissolved organic content from its initial concentration of 103 ± 2.4 to 84 ± 1.7 ppm. Sample B also appeared transparent (with a pale yellow color) after step 1 treatment with TOC reduction from 78 ± 1.5 to 66 ± 1.8 ppm. The low percent removal of the organics indicated poor removal efficiency of the lower molecular weight organics requiring further treatment using smaller pore size membranes.

Step 2 Treatment. Direct UF treatment of the raw field waters using the 50 kDa ceramic membrane resulted in a very low permeate flux. Figure 2 shows a comparison between DI-water flux as function of TMP for the 13 and 50 kDa PAN

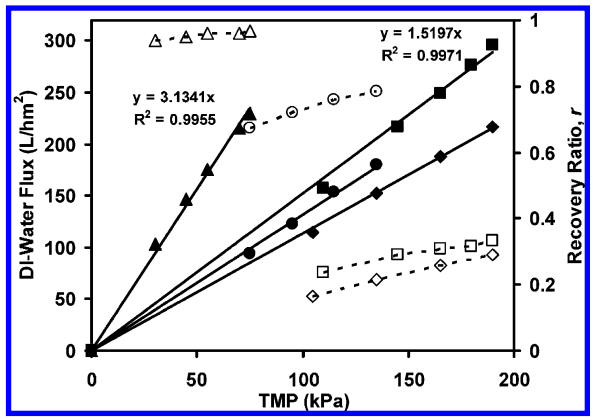

FIGURE 2. DI-water flux (solid symbols) and recovery ratio (open symbols) as functions of TMP for the (▲;△) 50 and (●;○) 13 kDa polymeric, and the (■;□) 50 and (◆;◇) 15 kDa ceramic membranes.

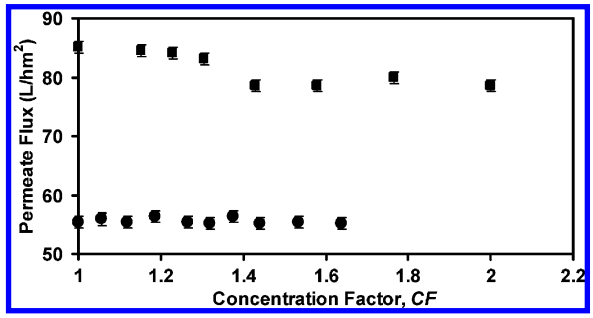

FIGURE 3. Step 2 batch-wise experiment using 50 kDa ceramic membrane for (■) sample A and (●) sample B (TMP = 150 kPa).

polymeric and the 15 and 50 kDa TiO_2 ceramic membranes. The values of the slopes indicate that the ceramic membrane of the same MWCO displays twice the resistance toward the flow of DI-water. Higher membrane resistance of the ceramic membrane may arise from its hydrophobic nature (*24*) as opposed to polymeric PAN membrane (*25*), a larger mean membrane pore length and/or a smaller mean membrane pore diameter. The 50 kDa ceramic membrane was used in step 2, since it may remove species with smaller molecular weight, especially if it possesses a smaller mean pore diameter compared with the same MWCO polymeric membrane used in step 1.

Figure 3 shows the permeate flux of step 2 treatment under constant TMP of 150 kPa as a function of concentration factor for samples A and B following step 1 treatment. The steady fluxes of approximately 78 and 55 L/hm^2 for samples A and B were achieved at concentration factors of 1.4 and 1, respectively. This indicates steady resistance from the polarized layer formed by the solutes carried from step 1 pretreatment (*8*). The higher flux of sample A may be attributed to its lower viscosity. Permeate from step 2 looked transparent and almost colorless, which suggests higher removal of large colloidal particles, as confirmed by DLS measurements. The TOC measurements showed that step 2 treatment could only remove about 4 ppm of organics in sample A and effectively no organics were removed from sample B. The relatively low percent rejection of the organics and the fact that completely transparent permeates were obtained after step 2 treatment, suggest that the organic contaminants are most likely water-soluble.

Results from step 1 and 2 treatments indicate that the physical treatment using UF alone was insufficient and thus MEUF tests were deemed necessary. In a third step the CPC

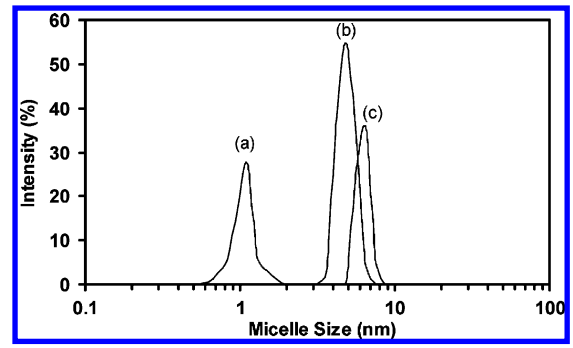

FIGURE 4. DLS measurements of micelle size of (a) 10 mM CPC, and a mixture of 10 mM CPC and permeate of step 2 for (b) sample A, and (c) sample B.

surfactant was added to the permeate from the second step in an attempt to remove the soluble organics. Prior to going forward, though, it was necessary to investigate the effect of the organic contaminants in the field samples on the CMC and the size of the CPC micelles.

Effect of the Organic Contaminants in the Field Samples on the CMC and Micellar Size of CPC. GC analyses of field samples A and B showed peaks at approximate retention times observed for naphthenic acids having carbon number between 7 and 10. The effect of naphthenic acids on the CMC and the size of the CPC micelles were detailed in our previous studies (*7, 8*). Surface tension measurements show that the CMC of CPC was reduced from 0.32 mM in DI-water to 0.07 mM in sample A, and to 0.08 mM in sample B. Moreover, DLS measurements showed that the average size of CPC micelles increased from 1 nm in DI-water to 6 nm in sample A and to 7 nm in sample B (Figure 4). This increase in the micelle size enabled the application of membranes with larger pore size, which, in turn, provided higher permeate flux. However, it should be noted that there exists an optimum pore size which prevents pore plugging and/or leakage of the micelles to the permeate side while providing high permeate fluxes (*8, 18*).

In the third step, 2 L of step 2 permeate, adjusted to 10 mM CPC, were used as feed in one-hour MEUF runs during which samples were drawn every 15 min. The average permeate concentration of CPC and the organic contaminants were reported at the corresponding TMPs.

Figure 5 (a) and (b) show the permeate flux and recovery ratio as functions of TMP for samples A and B, respectively, with the 13 kDa PAN and the 50 kDa ceramic membranes. The higher permeate flux from the polymeric PAN can be attributed to the relatively higher hydrophilicity of PAN in a hollow fiber structure module as well as the bigger effective surface area of the 13 kDa PAN membrane. Consequently, the polymeric membrane gave higher recovery ratios. On the other hand, higher percent rejections for the CPC and organic contaminants were achieved by the 50 kDa ceramic membrane as indicated in Table 2. It should be noted that regardless of the membrane type, MEUF treatment gave remarkably higher removal of the organics when compared to UF treatment.

It is evident from Table 2 that a higher percent rejection of CPC, and subsequently lower back contamination, was observed for the runs involving the field samples, that is, in the presence of contaminants, as opposed to 10 mM CPC in DI-water feed. In addition, the 50 kDa ceramic membrane was more effective in rejecting the organic contaminants at high TMPs, probably due to the nature of membrane material. In general, ceramic membranes are preferred by industry due to their high durability, high thermal resistance, and relatively easier cleaning protocols.

Modeling. The modified form of Darcy's law known as the resistance in series model, as shown in eq 5, was used

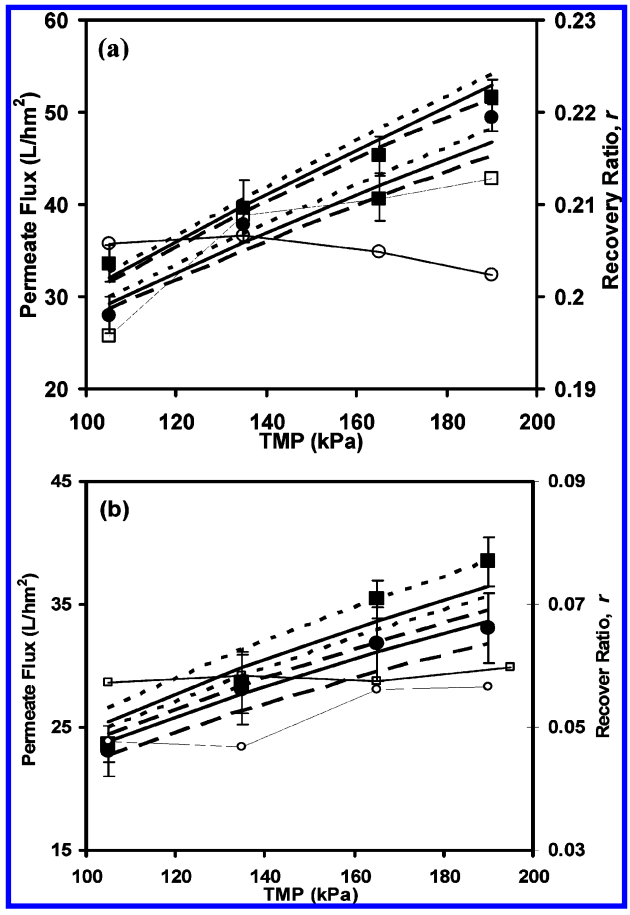

FIGURE 5. Permeate flux (solid symbols) and recovery ratio (open symbols) as functions of TMP for step 3 treatment using (a)13 kDa polymeric membrane, (b) 50 kDa ceramic membrane on (■;□) sample A, and (●;○) sample B {[CPC] = 10 mM in both samples, (—) model, (- -) β+10%, (- - -) β-10%; Points: experiments}.

to describe the flux decline during filtration processes (*11, 28–31*).

$$J = \frac{(\mathrm{TMP})}{\mu \sum R} \tag{5}$$

where J is the permeate flux in (m^3/m^2.sec) and μ is the viscosity of the feed solution in (Pa·sec) of the feed solution. The term ΣR stands for the sum of all the resistances obstructing the flow to the permeate side, including membrane resistance (R_m), internal pore plugging (R_{pp}), concentration polarization (R_c), gel layer (R_g), and the resistance caused when fouling occurs on the surface of the membrane (R_f) (*27, 32*). The intrinsic membrane resistance (R_m) is a property of the membrane and varies with membrane type, material and void fraction. The values of R_m are typically found from the slope of the flux versus TMP for DI-water (*28*), as shown in Figure 2. Resistance due to concentration polarization (CP) originates from the retention of solute material near the surface of the membrane. Although the cross-flow operation mode creates shear which limits the growth of the CP and gel layer, complete elimination of the CP layer is not possible. The existence of the CP layer leads to a continuous decline in the slope of the flux versus TMP as the TMP increases (*26*). Fouling, on the other hand, leads to a constant flux that is independent of the TMP (*29*). No such trend was observed in Figure 5. Therefore, R_f was eliminated from

TABLE 2. Percent Rejection and Average Permeate Concentration of CPC and Organic Contaminants Following Step 3 Treatment Using 13 kDa Polymeric and 50 kDa Ceramic Membranes for the Control Sample of 10 mM CPC and Samples A and B (CPC Was Added to Give [CPC] = 10 mM)

		13 kDa polymeric10 mM CPC (control sample)		50 kDa ceramic10 mM CPC (control sample)		13 kDa polymeric sample A in 10 mM CPC		50 kDa ceramic sample A in 10 mM CPC		13 kDa polymeric sample B in 10 mM CPC		50 kDa ceramic sample B in 10 mM CPC	
TMP(kPa)		CPC		CPC		CPC	organics	CPC	organics	CPC	organics	CPC	organics
105	$\%R_i$	96.90 ± 0.05		96.60 ± 0.06		98.10 ± 0.07	96.10 ± 0.05	99.70 ± 0.02	97.7 ± 0.1	97.70 ± 0.05	93.80 ± 0.55	98.2 ± 0.05	96.2 ± 0.1
	$[i]^a$	0.31 ± 0.01		0.34 ± 0.02		0.19 ± 0.01	2.70 ± 0.30	0.02 ± 0.01	1.8 ± 0.5	0.23 ± 0.03	4.32 ± 0.82	0.18 ± 0.06	2.7 ± 0.18
135	$\%R_i$	96.80 ± 0.01		96.40 ± 0.02		97.9 ± 0.1	94.20 ± 0.05	99.40 ± 0.03	98.1 ± 0.1	97.40 ± 0.04	84.10 ± 0.74	98.0 ± 0.04	91.3 ± 0.1
	$[i]^a$	0.32 ± 0.01		0.36 ± 0.02		0.20 ± 0.01	4.10 ± 0.12	0.06 ± 0.01	1.4 ± 0.4	0.26 ± 0.07	11.1 ± 0.6	0.25 ± 0.03	5.8 ± 0.41
165	$\%R_i$	96.70 ± 0.01		96.3 ± 0.02		97.60 ± 0.08	88.90 ± 0.04	98.60 ± 0.05	96.20 ± 0.05	96.10 ± 0.04	85.4 ± 0.2	97.5 ± 0.06	94.9 ± 0.05
	$[i]^a$	0.32 ± 0.01		0.37 ± 0.01		0.23 ± 0.01	8.4 ± 0.23	0.14 ± 0.05	2.90 ± 0.35	0.30 ± 0.02	10.25 ± 0.60	0.29 ± 0.05	3.5 ± 0.24
190	$\%R_i$	96.80 ± 0.01		95.80 ± 0.02		97.30 ± 0.05	80.90 ± 0.09	97.9 ± 0.04	95.80 ± 0.05	96.60 ± 0.02	79.50 ± 0.32	97.4 ± 0.76	92.3 ± 0.05
	$[i]^a$	0.31 ± 0.01		0.42 ± 0.03		0.26 ± 0.01	13.4 ± 0.81	0.21 ± 0.02	4.40 ± 0.74	0.34 ± 0.02	14.38 ± 0.46	0.31 ± 0.02	5.4 ± 0.12

[a] $[i]$ is the species average concentration in the permeate stream. [CPC] = mM, [organic contaminants] = ppm.

TABLE 3. Viscosities of the MEUF Feed Solutions

MEUF feed content	viscosity (Pa·s)
10 mM CPC (control sample)	0.00167 ± 0.00015
sample A mixed in 10 mM CPC	0.00355 ± 0.00014
sample B mixed in 10 mM CPC	0.00362 ± 0.00014

the model. Internal pore plugging occurs when the particle size of the solutes is smaller than the membrane pore diameter and is characterized by a significant decline in the permeate flux (*18*). This trend is not evident in Figure 5. Therefore, eq 5 reduces to eq 6 below.

$$J = \frac{(\mathrm{TMP})}{\mu(R_\mathrm{m} + R_\mathrm{c})} \tag{6}$$

The values of R_m for the 13 kDa polymeric PAN and the 50 kDa ceramic TiO_2 membranes were calculated from Figure 1 for DI-water and were found to be 2.77×10^{12} (1/m), 2.36×10^{12} (1/m), respectively. The viscosities of the different feed streams, μ, were independently measured and are listed in Table 3. R_c, on the other hand, changes with TMP according to a power law model as shown in eq 7 (*33*−*36*).

$$J = \frac{(\mathrm{TMP})}{\mu(R_\mathrm{m} + \beta(\mathrm{TMP})^n)} \tag{7}$$

The dimensionless compressibility index (n), which represents the manner a certain solute accumulates "compressed" on the surface of the membrane, was independently estimated from the batch experiments (*36*). Steady flux data, which were reached after about 2 h of the batch experimental runs, were used to estimate n. Accordingly, n was estimated to be 0.8 and the CP layer specific resistance, β, was a fitted parameter.

The model fit for the MEUF experiments using 13 kDa polymeric and for the 50 kDa ceramic membranes for both samples A and B are shown in Figure 5 (a) and (b), respectively. As shown in these figures, the model fits the data accurately for the two field samples and the two types of membranes with β as the only fitted parameter. The sensitivity analysis which is shown by 10% increase and decrease in β as indicated in Figure 5 (a) and (b) confirmed the relevance of the fitted parameter and that the value of β cannot be chosen randomly.

The feasibility of applying micellar-enhanced ultrafiltration using cetylpyridinium chloride (CPC) surfactant and polymeric or ceramic membranes for the removal of organic contaminants from field produced water samples was explored. A treatment train consisting of two-stage UF treatment followed by a third stage MEUF was able to remove free oil droplets, suspended solids and rejected more than 95% of the soluble organics and more than 98% of CPC. DLS and CMC measurements of CPC in the field samples showed appreciable decrease in CMC and increase in micelle size when compared with aqueous CPC solution. This important observation suggests that organic contaminants in fact contribute to improving MEUF. A mathematical model based on Darcy's law coupled with the resistance in-series model with variable CP layer resistance with only one fitted parameter described the flux trends for the two field water samples as well as the two membranes.

Acknowledgments

We thank the Natural Sciences and Engineering Research Council of Canada (NSERC) and the Center for Environmental Engineering Research and Education (CEERE) at the University of Calgary for their financial support. We also like to thank the reviewers for their valuable input.

Literature Cited

(1) Ali, S. A.; Henry, L. R.; Darlington, J. W.; Occapinti, J. New filtration process cut contaminants from offshore produced water. *Oil Gas J.* **1998**, *96*, 73–78.
(2) Chalaturnyk, R. J.; Scott, J. D.; özüm, B. Management of oil sands tailings. *Pet. Sci. Technol.* **2002**, *20*, 1025–1046.
(3) Veil, J. A.; Puder, M. G.; Elcock, D.; Redweik, R. J. A White Paper Describing Produced Water from Production of Crude Oil, Natural Gas and Coal Bed Methane; Prepared for U.S. Department of Energy: Washington, DC, 2004.
(4) Cline, J. T. Treatment and Discharge of Produced Water for Deep Offshore Disposal. presented at the API Produced Water Management Technical Forum and Exhibition, Lafayette, LA, 1998, 17−18.
(5) Quagraine, E. K.; Peterson, H. G.; Headley, J. V. In-situ bioremediation of naphthenic acids contaminated tailing pond waters in the Athabasca oilsands region-demonstration field studies and plausible options: A review. *J. Environ. Sci. Health* **2005**, *40*, 685–722.
(6) Allen, E. W. Process water treatment in Canada's oil sands industry: II. A review of emerging technologies. *J. Environ. Eng. Sci.* **2008**, *7*, 499–524.
(7) Deriszadeh, A.; Harding, T. G.; Husein, M. M. Improved MEUF removal of naphthenic acids from produced water. *J. Membr. Sci.* **2009**, *326*, 161–167.
(8) Deriszadeh, A.; Harding, T. G.; Husein, M. M. Role of naphthenic acid contaminants in the removal of p-xylene from synthetic produced water by MEUF. *Process Saf. Environ. Prot.* **2008**, *86*, 244–251.
(9) Purkait, M. K.; DasGupta, S.; De, S. Micellar-enhanced ultrafiltration of phenolic derivatives from their mixture. *J. Colloid Interface Sci.* **2005**, *285*, 395–402.
(10) Purkait, M. K.; DasGupta, S.; De, S. Micellar-enhanced ultrafiltration of eosin dye using hexadecyl pyridinium chloride. *J. Hazard. Mater. B* **2006**, *136*, 972–977.
(11) Purkait, M. K.; DasGupta, S.; De, S. Removal of dye from wastewater using micellar-enhanced ultrafiltration and recovery of surfactant. *Sep. Purif. Technol.* **2004**, *37*, 81–92.
(12) Purkait, M. K.; DasGupta, S.; De, S. Separation of aromatic alcohols using micellar-enhanced ultrafiltration and recovery of surfactant. *J. Membr. Sci.* **2005**, *250*, 47–59.
(13) Lee, J.; Yang, J. S.; Kim, H. J.; Baek, K.; Yang, J. W. Simultaneous removal of organic and inorganic contaminants by micellar enhanced ultrafiltration with mixed surfactants. *Desalination* **2005**, *184*, 395–407.
(14) Yang, J. S.; Baek, K.; Yang, J. W. Crossflow ultrafiltration of surfactant solution. *Desalination* **2005**, *184*, 385–394.
(15) Juang, R. S.; Xu, Y. Y.; Chen, C. L. Separation and removal of metal ions from dilute solutions using micellar-enhanced ultrafiltration. *J. Membr. Sci.* **2003**, *218*, 257–267.
(16) Jadhav, S. R.; Verma, N.; Sharma, A.; Bhattacharya, P. K. Flux and retention analysis during Micellar-enhanced ultrafiltration for the removal of phenol and aniline. *Sep. Purif. Technol.* **2001**, *24*, 541–557.
(17) Fillipi, B. R.; Brant, L. W.; Scamehorn, J. F.; Christian, S. D. Use of Micellar enhanced ultrafiltration at low surfactant concentrations and with anionic-nonionic surfactant mixtures. *J. Colloid Interface Sci.* **1999**, *213*, 68–80.
(18) Markels, J. H.; Lynn, S.; Radke, C. J. Cross-flow ultrafiltration of micellar surfactant solutions. *AIChE J.* **1995**, *41*, 2058–2066.
(19) Dunn, R. O.; Scamehorn, J. F.; Christan, S. D. Simultaneous removal of dissolved organics and divalent metal ions from wastewater using micellar-enhanced ultrafiltration. *Colloids Surf.* **1989**, *35*, 49–56.
(20) Dunn, R. O.; Scamehorn, J. F.; Christan, S. D. Use of micellar-enhanced ultrafiltration to remove dissolved organics from aqueous streams. *Sep. Sci. Technol.* **1985**, *20*, 257–284.
(21) Li, C.-W.; Liu, C.-K.; Yen, W.-S. Micellar-enhanced ultrafiltration (MEUF) with mixed surfactants for removing Cu(II) ions. *Chemosphere* **2006**, *63*, 353–358.
(22) Bielska, M.; Szymanowski, J. Micellar-enhanced ultrafiltration of nitrobenzene and 4-nitrophenol. *J. Membr. Sci.* **2004**, *243*, 273–281.
(23) Tung, C.-C.; Yang, Y.-M.; Chang, C.-H.; Maa, J.-R. Removal of copper ions and dissolved phenol from water using micellar-enhanced ultrafiltration with mixed surfactants. *Waste Manage.* **2002**, *22*, 695–701.

(24) Hiromi, Y.; Shinichi, K.; Shuai, Y.; Kazuhiro, M.; Masakazu, A.; Michio, M. Efficient adsorption and photocatalytic degradation of organic pollutants diluted in water using the fluoride-modified hydrophobic titanium oxide photocatalysts: Ti-containing Beta zeolite and TiO2 loaded on HMS mesoporous silica. *Catal. Today* **2007**, *126*, 375–381.
(25) Jung, B. Preparation of hydrophilic polyacrylonitrile blend membranes for ultrafiltration. *J. Membr. Sci.* **2004**, *229*, 129–136.
(26) Bacchin, P.; Si-Hassen, D.; Starov, V.; Clifton, J.; Aimar, P. A unifying model for concentration polarization, gel-layer formation and particle deposition in cross-flow membrane filtration of colloidal suspensions. *Chem. Eng. Sci.* **2002**, *57*, 77–91.
(27) Field, R. W.; Wu, D.; Howell, J. A.; Gupta, B. B. Critical flux concept for micro filtration fouling. *J. Membr. Sci.* **1995**, *100*, 259–272.
(28) Juang, R.-S.; Chen, H.-L.; Chen, Y.-S. Resistance-in-series analysis in cross-flow ultrafiltration of fermentation broths Bacillus subtilis culture. *J. Membr. Sci.* **2008**, *323*, 193–200.
(29) Rai, P.; Rai, C.; Majumdar, C. G.; DasGupta, S.; De, S. Resistance in series model for ultrafiltration of mosambi (*Citrus sinensis* (L.) Osbeck) juice in a stirred continuous mode. *J. Membr. Sci.* **2006**, *283*, 116–122.
(30) Tansel, B.; Bao, W. Y.; Tansel, I. N. Characterization of fouling kinetics in ultrafiltration systems by resistances in series model. *Desalination* **2000**, *129*, 7–14.
(31) Cheng, T. W.; Yeh, H. M.; Gau, C. T. Resistance analyses for ultrafiltration in tubular membrane module. *Sep. Sci. Technol.* **1997**, *32*, 2623–2640.
(32) Davis, R. H.; Leighton, D. T. Shear-induced transport of a particle layer along a porous wall. *Chem. Eng. Sci.* **1987**, *42*, 275–281.
(33) Boerlage, S. F. E.; Kennedy, M. D.; Aniye, M. P.; Abogrean, E.; Tarawneh, Z. S.; Schippers, J. C. The MFI-UF as a water quality test and monitor. *J. Membr. Sci.* **2003**, *211*, 271–289.
(34) Carrère, H.; Blaszkow, F.; Roux de Balmann, H. Modelling the clarification of lactic acid fermentation broths by cross-flow microfiltration. *J. Membr. Sci.* **2001**, *186*, 219–230.
(35) Piron, E.; René, F.; Latrille, E. A cross-flow microfiltration model based on integration of the mass transport equation. *J. Membr. Sci.* **1995**, *108*, 57–70.
(36) Nakanishi, K.; Tadokoro, T.; Matsuno, R. On the specific resistance of cakes of microorganisms. *Chem. Eng. Commun.* **1987**, *62*, 187–201.

ES902862J